A Broadband Unidirectional Twin-slot Array using Phase Cancellation with a Compact Backing Ground Reflector

Michael Simcoe, Raviraj S. Adve, Meide Qiu and George V. Eleftheriades,
The Edward S. Rogers Dept. of Electrical and Computer Engineering,
University of Toronto, Toronto, ON M5S 3G4, Canada

***Abstract*—This paper examines the feasibility of using the phase cancellation technique with an electrically small ground plane. A modified broadband twin slot structure fed by a corporate microstrip feed on an electrically thin substrate is made unidirectional by using a backing ground reflector. The coupling to the quasi-TEM mode is reduced through a phase cancellation technique by placing the twin elements at a distance of about half a guided wavelength. Traditional designs employing phase cancellation used an electrically large ground plane, typically about $2.5\lambda_o$ from each slot edge to the ground plane edge. In this work, it is demonstrated that a ground plane that is only $0.5\lambda_o$ from each slot edge actually achieves smoother radiation patterns and higher gain. The proposed structure maintains its primary characteristics over the large impedance match bandwidth of the antenna (18%). The total size is about $1.6\lambda_o x 1.6\lambda_o x 0.25\lambda_o$. As a result of the reduced overall size compared to previous implementations, this structure could be useful in numerous wireless applications. This study is verified experimentally at a nominal design frequency of 8GHz.**

***Index Terms*—Broadband antenna, phase cancellation, slot antenna.**

I. Introduction

PLANAR slot antennas have various applications due to their broad bandwidth and low profile. However, slots on an electrically thin substrate radiate from both sides of the substrate. This is an undesirable characteristic in many applications because it reduces the forward gain. A classic technique to reduce or eliminate the back radiation has been to place a cavity behind the slot [1]. However, this approach increases the construction complexity considerably due to the additional machining and attaching of the cavity to the antenna as well as any subsequent tuning.

Another effective approach to reduce the back radiation in a planar slot array environment is to place a backing ground reflector at a distance of $\lambda_0/4$ away from the slot ground plane [2]. By placing the backing ground reflector, a TEM or quasi-TEM mode can then be supported in the space created between the slot ground plane and the backing ground reflector. To reduce the power coupled to this mode, the slots in the array are spaced at a distance close to half a guided wavelength apart such that the power radiated by adjacent slots adds destructively. This general approach is termed phase cancellation and finds application in the reduction of power coupled to surface-waves on electrically thick substrates [3] as well as in the reduction of power coupled to TEM or quasi-TEM modes as in this application. A more detailed background into the development of phase cancellation for different applications can be found in [4].

Many antenna applications require a large operating bandwidth in terms of impedance match, radiation pattern shape, and gain. Additionally, these characteristics should be met with as compact and inexpensive an antenna as possible. Another planar antenna structure that achieves broadband unidirectional radiation patterns is the aperture coupled stacked patch [5]. However, this approach requires multiple substrate layers that must be carefully aligned and glued, increasing the complexity and cost. Using the approach presented here, only a single substrate is needed. The backing ground reflector is simply placed at a distance of about $0.25\lambda_o$ and does not require any additional alignment. Also, compared with previous implementations of the phase cancellation approach with twin slot type structures [6], this antenna is more broadband and the total size is much smaller at only $1.6\lambda_o x 1.6\lambda_o x 0.25\lambda_o$ (the smallest ground plane used in [6] was about $4\lambda_o x 4\lambda_o x 0.25\lambda_o$ – corresponding to a 60% reduction in the overall antenna size).

The purpose of this study is to demonstrate the feasibility of using the phase cancellation approach with an electrically compact ground plane. The phase cancellation approach is broadband if the slot elements are kept in phase as is done here using a corporate feed network. It will be demonstrated that a compact backing ground reflector with a broadband twin slot geometry achieves smooth radiation patterns and high gain over the entire match bandwidth. The proposed antenna structure will be compared to the same antenna structure on an electrically large ground plane and it will be shown to be superior in terms of both radiation pattern and gain performance.

This work was supported in part by the U.S. Department of Defense under the CHSSI program.

This paper is organized as follows. In Section II, the basic principle of operation of the proposed array is outlined, including a brief review of the phase cancellation approach and the design of the twin slot geometry. In Section III, the experimental radiation patterns and gain are compared for the twin slot structure on the electrically large and electrically small ground plane. Finally, in Section IV some conclusions are discussed.

II. PRINCIPLE OF OPERATION

A. Theory

In this section, since a comprehensive treatment of the phase cancellation approach is given in [7,8], only a brief review of the approach and the primary results will be given. The side profile geometry of a generic twin slot array type structure is shown in Figure 1. In this figure, P_{RAD} is the power radiated to free space, P_{SW} is the power lost to surface waves, and P_{BACK} is the power coupled to the mode that propagates between the two ground planes. This parallel plate mode is treated here as a TEM mode since the substrate on the top ground plane is electrically very thin ($h=0.01\lambda_0$) in this application.

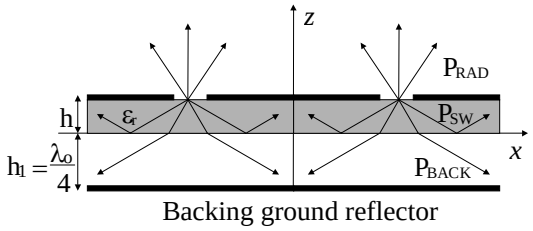

Figure 1: Side profile geometry of a generic twin slot array structure.

This antenna will have an efficiency given by

$$\eta = \frac{P_{RAD}}{(P_{RAD} + P_{SW} + P_{BACK})}. \tag{1}$$

For a general slot current distribution, within an N-slot array, the far-field patterns and the radiated power are given by [7]

$$E_\theta(r,\theta,\varphi) = j\frac{\exp(-jk_0 r)}{2\pi r} k_0 \times \left[\frac{\sin\varphi}{d_{TM}} I_{RMx}(\theta,\varphi) - \frac{\cos\varphi}{d_{TM}} I_{RMy}(\theta,\varphi)\right] \exp(jk_0\cos\theta) \tag{2}$$

$$E_\varphi(r,\theta,\varphi) = j\frac{\exp(-jk_0 r)}{2\pi r} k_0 \cos\theta \times \left[\frac{\cos\varphi}{d_{TE}} I_{RMx}(\theta,\varphi) + \frac{\sin\varphi}{d_{TE}} I_{RMy}(\theta,\varphi)\right] \exp(jk_0\cos\theta) \tag{3}$$

where

$$I_{RMx}(\theta,\varphi) = \int_{y'}\int_{x'} M_x(x',y') \times \exp[jk_0(x'\sin\theta\cos\varphi + y'\sin\theta\sin\varphi)]dx'dy' \tag{4}$$

and

$$I_{RMy}(\theta,\varphi) = \int_{y'}\int_{x'} M_y(x',y') \times \exp[jk_0(x'\sin\theta\cos\varphi + y'\sin\theta\sin\varphi)]dx'dy' \tag{5}$$

and the variables are defined by

$$d_{TM} = j\eta_{TM}\sin\psi + \cos\psi, \quad d_{TE} = j\eta_{TE}\sin\psi + \cos\psi \tag{6}$$

$$\eta_{TM} = \frac{\cos\theta_i}{\sqrt{\varepsilon_r}\cos\theta}, \quad \eta_{TE} = \frac{\cos\theta}{\sqrt{\varepsilon_r}\cos\theta_i} \tag{7}$$

$$\psi = k_0\sqrt{\varepsilon_r}\, h\cos\theta_i \tag{8}$$

$$\sin\theta = \sqrt{\varepsilon_r}\sin\theta_i \tag{9}$$

The radiated power is then given by

$$P_{RAD} = \frac{1}{2\eta_0}\int_0^{2\pi}\int_0^{\frac{\pi}{2}} (|E_\theta|^2 + |E_\varphi|^2)\, r^2 \sin\theta d\theta d\varphi \tag{10}$$

The power lost to surface waves is

$$P_{SW} = \frac{\omega\varepsilon}{8\pi h_{eff}}\int_0^{2\pi} \left|-\sin\varphi\, I_{SMx}(\varphi) + \cos\varphi\, I_{SMy}(\varphi)\right|^2 d\varphi \tag{11}$$

where

$$I_{SMx}(\varphi) = \int_{y'}\int_{x'} M_x(x',y')\exp[j\beta(x\cos\varphi + y\sin\varphi)]dx'dy' \tag{12}$$

$$I_{SMy}(\varphi) = \int_{y'}\int_{x'} M_y(x',y')\exp[j\beta(x\cos\varphi + y\sin\varphi)]dx'dy' \tag{13}$$

Finally, the power coupled to the TEM parallel plate mode is

$$P_{BACK} = \frac{k_0}{16\pi\eta h_1}\int_0^{2\pi} \left|\sin\varphi\, I_{PMx}(\varphi) - \cos\varphi\, I_{PMy}(\varphi)\right|^2 d\varphi \tag{14}$$

where

$$I_{PMx}(\varphi) = \int_{y'}\int_{x'} M_x(x',y') \times \exp[jk_0(x\cos\varphi + y\sin\varphi)]dx'dy' \tag{15}$$

$$I_{PMy}(\varphi) = \int_{y'}\int_{x'} M_y(x',y') \times \exp[jk_0(x\cos\varphi + y\sin\varphi)]dx'dy' \tag{16}$$

B. Geometry and design

These general results must be applied to the particular current distribution of the modified twin slot geometry explored in this study. The geometry of one of slots along with the dimensions used is given in Figure 2 while the layout of the twin slot structure is given in Figure 3. This structure is essentially a modification of the microstrip T-fed slot antenna described in [9]. However, by simulation of the structure in [9], it was determined that its exact impedance behavior is sensitive to the positioning of the strip with respect to the slot. To alleviate the tolerances on the alignment of the masks on the two sides of the substrate, the strip is placed on the top side within the slot boundary itself. This ensures proper positioning of the strip with respect to the slot since the strip

and slot appear on the same mask. The strip is then attached to the microstrip feedline with a via similar to that used in [10]. Examining the slot/strip structure as implemented here and comparing to [9,10], it seems that the structure essentially appears as a via fed folded slot. The offset strip enhances the impedance bandwidth through the introduction of additional resonances. To design this twin slot structure and microstrip feed network, a '2.5-D' (where all planar surfaces are assumed infinite in the transverse direction) Method of Moments (MoM) commercial software package was used. The return loss for the designed twin slot structure is given in Figure 4. The nominal design center frequency is 8GHz.

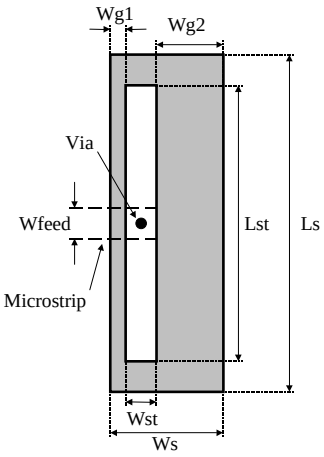

Figure 2: Microstrip-fed offset folded slot geometry. The final dimensions used for the twin slot design are (in microns): Ws=5015, Ls=16634, Wst=1188, Lst=12984, Wg1=112, Wg2=3715, Wfeed=1280, Dvia=250.

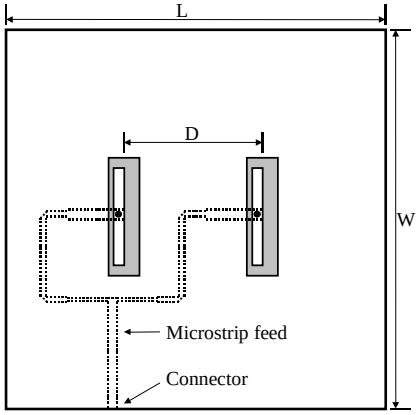

Figure 3: Layout of the twin slot geometry. The backing ground reflector lies directly underneath at a distance of h1 and has the same outer dimension W and L. The center-to-center distance between the slots is D=0.54λ=20250μm.

Given the complexity of this geometry, a determination of the exact current distribution in a closed form expression appropriate for the equations above is difficult. As such, the current distribution will be approximated to obtain the efficiency and gain and compared to the results obtained numerically by the 2.5-D MoM simulator. Since the slot appears to operate like a folded slot, the current distribution is assumed to be that of a half-wave slot (co-sinusoidal) with a width equal to that of the entire slot. The results of the comparison between theory and the 2.5-D MoM simulation data for the efficiency, gain, and E and H plane radiation patterns are given in Figure 5 through Figure 8. As seen, there is good agreement between the theoretical and numerical results, implying that the approximated current distribution is reasonably accurate.

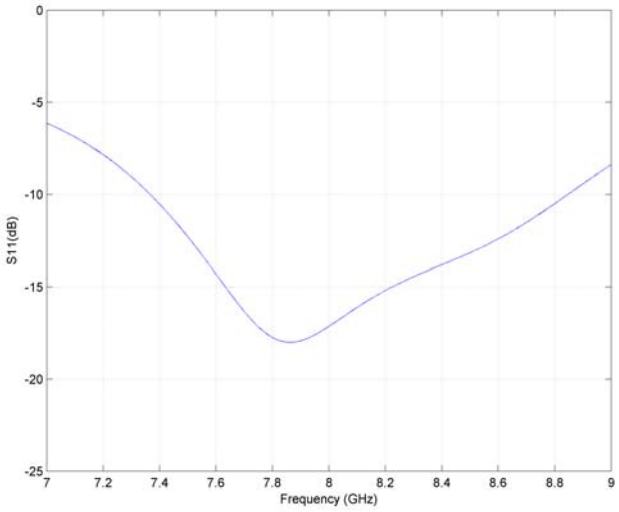

Figure 4: The 2.5-D MoM simulated return loss for the designed antenna.

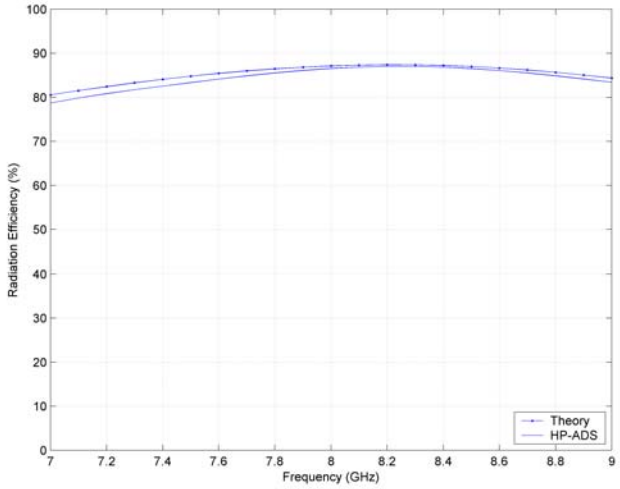

Figure 5: The 2.5-D MoM simulated and theoretical efficiency for the designed antenna.

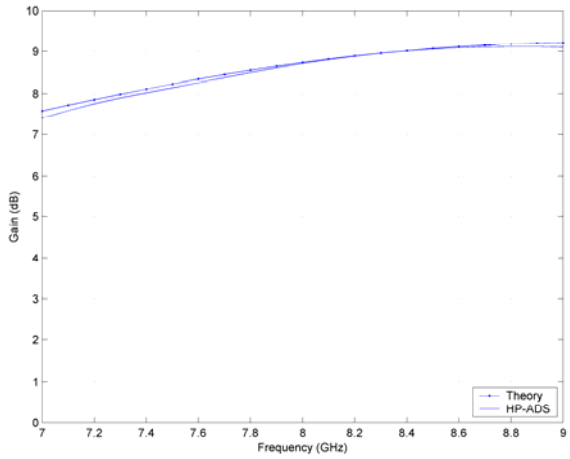

Figure 6: The 2.5-D MoM simulated and theoretical gain for the designed antenna.

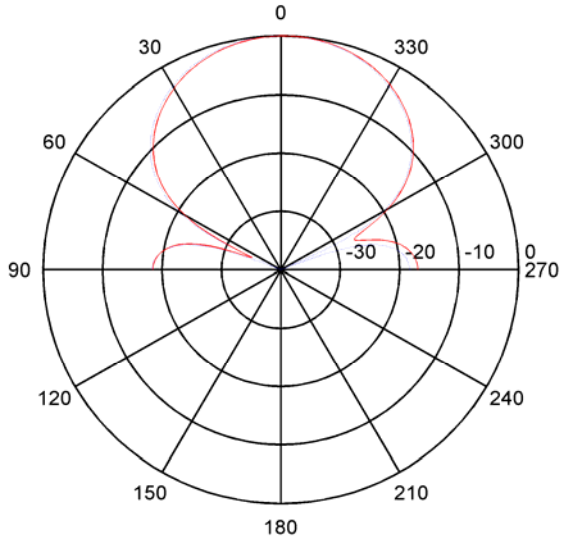

Figure 7: The 2.5-D MoM simulated and theoretical E-plane co-polarized radiation pattern at the design frequency of 8GHz. Solid line: 2.5-D MoM; dotted line: theory.

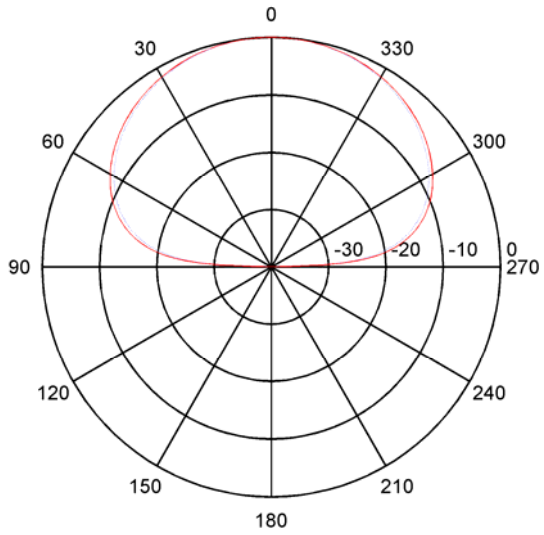

Figure 8: The 2.5-D MoM simulated and theoretical H-plane co-polarized radiation pattern at the design frequency of 8GHz. Solid line: 2.5-D MoM; dotted line: theory.

C. Finite ground plane effects

However, in regards to the previous section, it must be observed that the 2.5-D MoM simulated substrate and ground plane are assumed to be infinite in the transverse direction. As such, any power coupled to the surface wave or parallel plate mode simply disappears. In reality, uncancelled surface wave or parallel plate mode power will diffract off the edges of the finite substrate and ground plane and cause radiation pattern interference and hence affect the gain [11]. This effect will also be shown to have a significant effect in the experimental section.

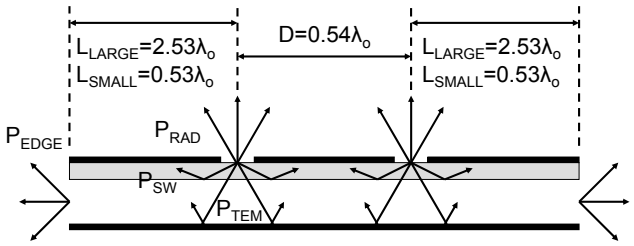

Figure 9: Geometry of large and small substrates antenna.

The dimensions of the large and small substrate antenna are shown in Figure 9 from which the basic operation of this antenna can be understood. The uncancelled surface wave and parallel plate mode power will radiate from the edges of the finite substrate, labeled as P_{EDGE} in Figure 9. For the small substrate case, since the edges are located at about half a free space wavelength from the slot edges, some of the power radiated at the edges of the substrate will add in-phase with the main beam. That is, the power radiated at the edges of the substrate essentially acts as part of the twin slot array. Of course, since this is diffracted power, some of the radiation

will also appear behind the backing ground reflector. So if the power coupled to the parallel plate mode were large (for example, if a single slot was used instead of twin slots), the back radiation level will increase. For the large substrate case, since the power radiated at the opposite edges of the substrate are located far away from each other, the radiation pattern from these edges will form grating lobes that superimpose on the twin slot array's pattern. The alternating constructive and destructive nature of the grating lobes will thereby cause ripples and distortion in the overall radiation pattern. According to this description, one would expect to see distortion and ripples for the large substrate case and comparatively smoother patterns and higher gain for the smaller substrate case. These effects will be demonstrated in the next section.

III. Experimental and Numerical Results

A. *Electrically large ground plane results*

In this section, the results are given for the twin slot structure on an electrically large ground plane. Referring to Figure 3, the outer dimensions of the substrate and ground planes are WxL=21cmx21cm ($5.6\lambda_0$x$5.6\lambda_0$). The measured and 2.5-D MoM simulated return loss are given in Figure 10. The observed deviation in the return loss is likely a result of variations in the etched antenna dimensions and via placement, and possibly a difference in the actual and reported substrate permittivity. The –10dB return loss bandwidth is between 7.2GHz to 8.8GHz, so with a nominal center frequency of 8GHz the fractional bandwidth is 18.8%.

The measured radiation patterns are compared to those obtained from a commercial full 3-D MoM based simulation tool [12] so that the effect of the scattering from the finite ground plane will be included. A 2.5-D MoM tool is used for design since the assumption of an infinite substrate simplifies the MoM calculation considerably. Since the structures analyzed are electrically large, the corporate feed network is omitted in the 3-D MoM analysis to reduce the number of unknowns and permit manageable runtimes. Each slot is individually fed with a length of microstrip having the same width as was designed (see W_f in Figure 2). The measured radiation patterns are compared to the 3-D MoM radiation patterns at the designed center frequency of 8GHz for the E and H plane co-polarized patterns in Figure 11 and Figure 12 respectively.

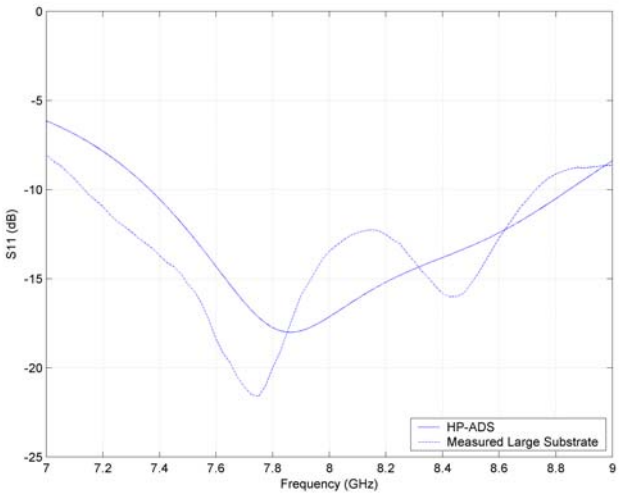

Figure 10: Large substrate measured and 2.5D MoM simulated return loss. Solid line: 2.5-D MoM; dotted line: measured.

As observed, the remaining uncancelled parallel plate mode power is scattered from the edges of the finite ground plane and interferes with the radiation pattern. A similar effect was observed in [11] for uncancelled surface wave power. This interference manifests itself as ripples in the radiation pattern, resulting in an undesirable randomized spatial gain variation. This effect is even more pronounced at some other frequencies. The E-plane co-polarized pattern is also shown at the two end point of the –10dB return loss bandwidth (7.2GHz and 8.7GHz) in Figure 13. While the pattern is relatively smooth at the low end of the frequency range near 7.2GHz, the ripples (distortion) in the radiation pattern are strong near the high frequency end point (8.7GHz) causing significant gain degradation.

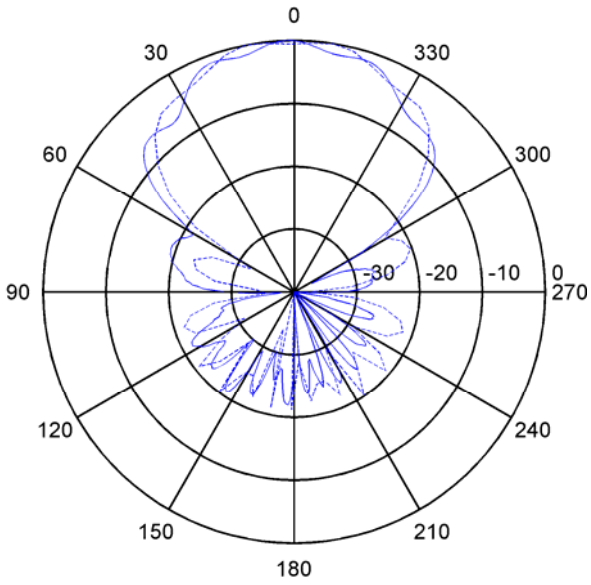

Figure 11: Large ground plane measured and 3-D MoM simulated E-plane co-polarized radiation pattern at the design frequency of 8GHz. Solid line: 3-D MoM; dotted line: measured.

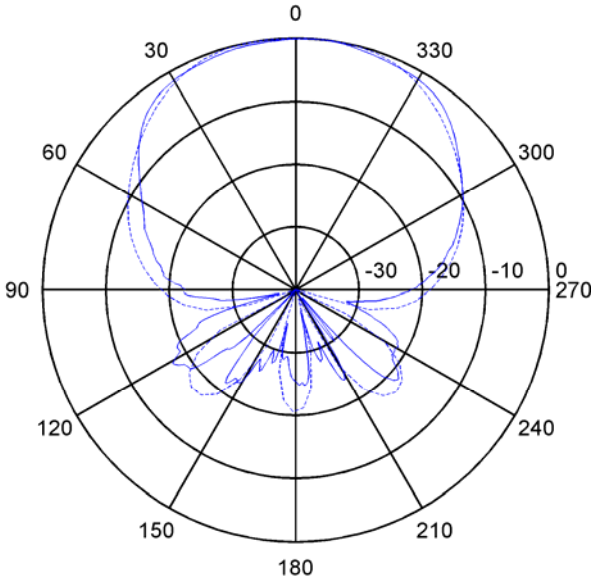

Figure 12: Large ground plane measured and 3-D MoM simulated H-plane co-polarized radiation pattern at the design frequency of 8GHz. Solid line: 3-D MoM; dotted line: measured.

Making meaningful gain measurements with a distorted beam is problematic since the gain varies strongly between the peaks and troughs of the radiation pattern. As a result of these strong variations, the measured gain is always taken at broadside to the array using the gain comparison method [13]. If there happens to be a peak (constructive interference) or a trough (destructive interference) at broadside at a particular frequency, the gain would read higher or lower respectively.

The resulting measured absolute gain within the –10dB impedance bandwidth is shown in Figure 14. As shown, the gain drops off sharply near the high end of the impedance match bandwidth (near 8.7GHz) as a result of the significant radiation pattern distortion near that point. The average gain of this antenna over this bandwidth is 7.3dB.

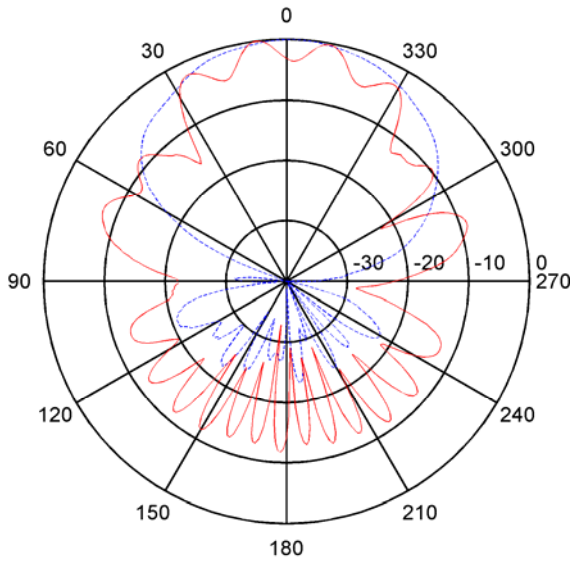

Figure 13: Large ground plane measured E-plane co-polarized radiation pattern at the end points of the impedance match bandwidth. Dotted line: 7.2GHz; solid line: 8.7GHz.

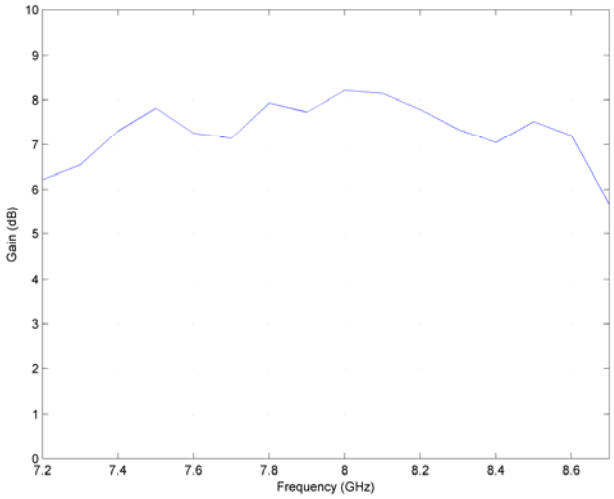

Figure 14: Broadside measured absolute gain for the large ground plane antenna.

The primary conclusion for the large substrate antenna is that due to the ripples in the pattern, even at the center frequency and particularly at the higher end of the frequency band, this antenna has several significant undesirable characteristics. As will be demonstrated in the next section, these characteristics are not observed for the same antenna on a compact ground plane.

B. Electrically small ("compact") substrate results

In this sub-section, the results for the twin slot structure on the electrically small (compact) substrate are given. Referring

to Figure 3, the outer dimensions of the substrate and ground planes are W×L=6cmx6cm ($1.6\lambda_0$x$1.6\lambda_0$). In order to keep everything the same for the purpose of direct comparison, the same antenna was used again. That is, the larger substrate and backing ground reflector were simply cut down to this smaller size. The measured return loss for the small and large ground plane structures are shown in Figure 15. As observed, the absolute bandwidth remains the same (from 7.2GHz to 8.7Ghz) while the shape does change somewhat. A possible explanation for this is a small change in the backing ground reflector height compared to the large ground plane when reattaching it, or that since the backing ground reflector is now electrically small, the backing ground reflector itself may be introducing an additional resonance. In any case, the change isn't significant since the same absolute bandwidth is maintained still giving a fractional bandwidth of 18.8%.

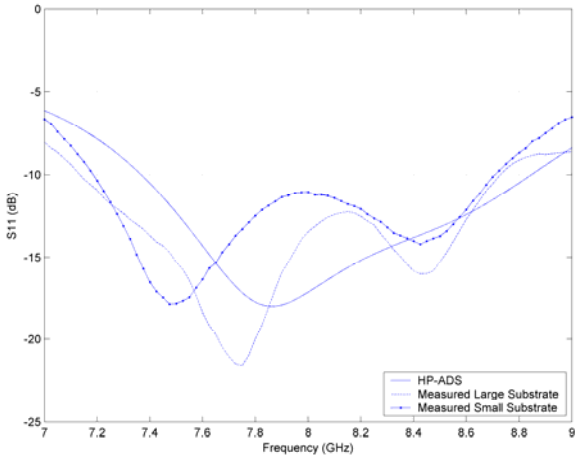

Figure 15: Measured return loss for the large and compact ground plane configurations compared to the 2.5-D MoM simulation.

The measured radiation patterns are compared to those obtained from the same commercial full 3-D MoM based simulation tool [12] used before for the large substrate so that the effect of the scattering from the finite ground plane will be included. The measured E and H plane co-polarized radiation patterns are compared to the 3-D MoM radiation patterns at the designed center frequency of 8GHz in Figure 16 and Figure 17 respectively.

In contrast to the results obtained for the large substrate, these radiation patterns are relatively smooth and undistorted despite having an electrically smaller ground plane. The measured E-plane co-polarization is shown near the two end points of the –10dB match bandwidth (7.2GHz and 8.7GHz) in Figure 18. Once again the patterns are smooth and undistorted compared to the large substrate. There is some asymmetry present in the patterns, partially due to the asymmetry in the corporate feed arrangement, and partially due to the electrically close proximity of the connector to the slot array (see Figure 20).

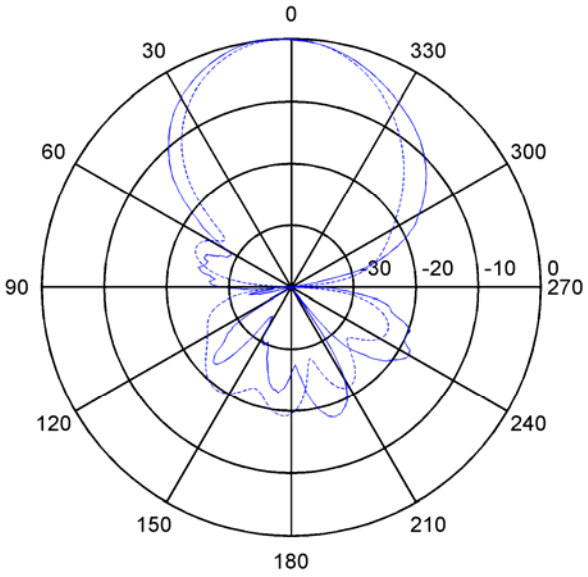

Figure 16: Compact ground plane measured and 3-D MoM simulated E-plane co-polarized radiation pattern at the design frequency of 8GHz. Solid line: 3-D MoM; dotted line: measured

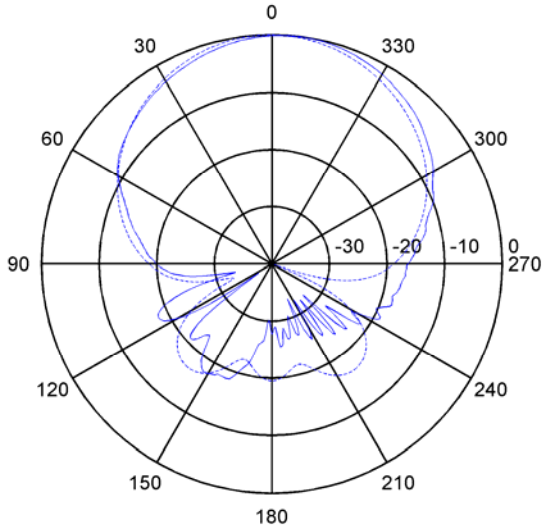

Figure 17: Compact ground plane measured and 3-D MoM simulated H-plane co-polarized radiation pattern at the design frequency of 8GHz. Solid line: 3-D MoM; dotted line: measured

For the purposes of making a direct comparison, the gain is again measured broadside to the array using the gain comparison method. The resulting measured absolute gain over the –10dB impedance match bandwidth is shown in Figure 19. As shown, the gain variation is smoother compared to the large ground plane case since the radiation pattern distortion is lower. The average gain of this antenna over this bandwidth is 8.5dB. The compact antenna has a higher gain than the larger antenna because the feedline losses are reduced and because the some of the power radiated at the edges of the

substrate adds in phase with the main beam, thereby avoiding the distortion seen with the large substrate case.

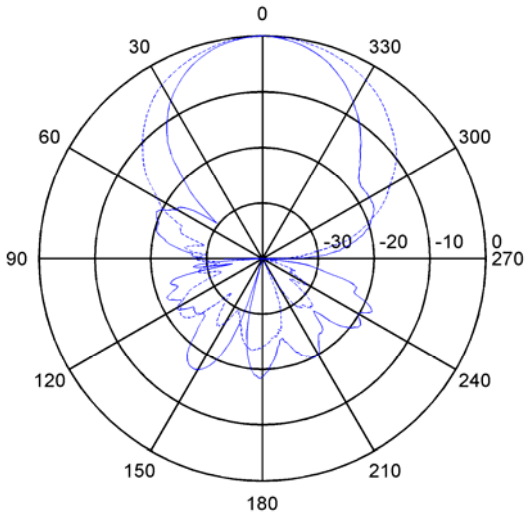

Figure 18: Compact ground plane measured E-plane co-polarized radiation pattern measured at the end points of the impedance match bandwidth. Dotted line: 7.2GHz; solid line: 8.7GHz.

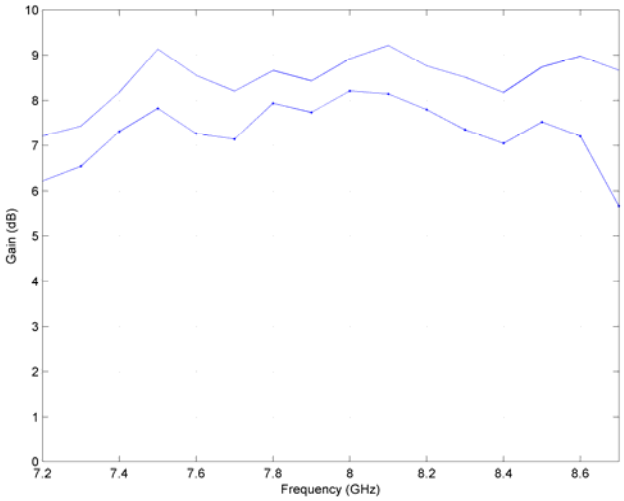

Figure 19: Broadside measured absolute gain for the large and compact ground plane antenna. Solid line: compact; dotted line: large.

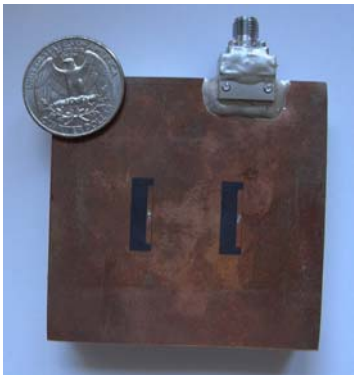

Figure 20: Photograph of the prototype twin slot antenna with a compact ground plane.

The primary conclusion for the compact ground plane antenna compared to the large ground plane antenna is that the radiation patterns are smoother and the average gain is higher. Also, the total antenna size is smaller, which is highly desirable in many applications.

IV. Conclusion

A broadband unidirectional twin slot antenna has been presented. The phase cancellation approach was used successfully to reduce the coupling to the parallel plate mode, despite the significantly smaller ground plane size compared with previous implementations. It was demonstrated that the structure actually has better performance in terms of pattern clarity and gain when implemented on the compact ground plane compared to a larger ground plane version. This was verified both through simulation and direct comparison experiment. As a result of the reduced overall size ($1.6\lambda_0 x 1.6\lambda_0 x 0.25\lambda_0$), this design makes the phase cancellation more readily applicable.

Acknowledgment

References

[1] "Cavity backed slot antenna" etc. Will find.
[2] M. Qiu, M. Simcoe, and G.V. Eleftheriades, "Radiation efficiency of printed slot antennas backed by a ground reflector," *IEEE AP-S Int. Symp. Dig.*, Salt Lake City, UT, July 2000, pp.1612-1615 .
[3] R.L. Rogers and D.P. Neikirk, "Use of broadside twin element antenna to increase efficiency on electrically thick substrate substrates," *Int. J. Infrared Millimeter Waves*, vol. 9, no. 11, pp. 949-969, 1988.
[4] D.B. Rutledge, D.P. Neikirk, and D.P.Kasilingam, "Integrated circuit antennas," in Infrared and Millimeter Waves, K.J. Button, Ed. New York Academic, 1983, vol. 10, pp. 1-90.
[5] J.F. Zurcher and J.F. Gardiol "Broadband patch antennas," Artech House, Boston, 1995.
[6] M. Qiu and G.V. Eleftheriades, "Highly efficient unidirectional twin arc-slot antennas on electrically thin substrates," *IEEE Trans. Antennas Propagat.*, vol. 52, pp. 53-58, Jan. 2004.
[7] G.V. Eleftheriades and M. Simcoe, "Gain and efficiency of linear slot arrays on thick substrates for millimeter-wave wireless applications," IEEE AP-S Int. Symp. Dig., Orlando, FL, July 1999, pp. 2428-2431.
[8] G.V. Eleftheriades and M. Qiu, "Efficiency and gain of slot antennas and arrays on thick dielectric substrates for mm-wave applications: A unified approach," *IEEE Trans. Antennas Propagat.*, vol. 50, pp. 1088-1098, Aug. 2000.
[9] Y.W. Jang, "Broadband cross-shaped microstrip-fed slot antenna", *Electronic Letters*, vol. 36, no. 25, Dec. 2000.
[10] W.R. Deal, V. Radisic, Q. Yongxi, T. Itoh, "A broadband microstrip-fed slot antenna," *IEEE MTT-S Symposium*, pp.21-24, 1999.
[11] M. Qiu, M. Simcoe, and G.V. Eleftheriades, "High-gain meander-less slot arrays on electrically thick substrates at mm-wave frequencies," *IEEE Trans. Microwave Theory Tech.*, vol. 50, pp. 517-528, Feb.2002.
[12] B.M. Kolundzija, B.D. Popovic, T.K. Sarkar, R.F. Harrington, WIPL-D Professional Version. 2000, OHRN Enterprises: Dewitt, NY.
[13] W.H. Kummer and E.S. Gillespie, "Antenna measurements-1978," *Proc. IEEE*, vol. 66, pp. 483-507, Apr.1978.

Michael Simcoe.